

Climate Change and Phenological Shifts in Hessian Deciduous Forests: A Two-Decade NDVI Analysis

Konstantin Engelmayer, Malte Vandamme

March 2024

Abstract

Climate change, driven by human activities, markedly influences plant phenology, signaling shifts in the timing of natural events. This research delves into the phenological changes of Hessian deciduous broadleaf forests, employing NDVI data from MODIS to span the years 2000 to 2023. Our findings reveal a significant trend: leaf emergence in spring has advanced by approximately 1.82 days per decade, while the season's end has been delayed by about 1.08 days per decade. This study builds upon existing literature, examining the interplay between the onset of spring and the end of the growing season, a relationship found to be subtly correlated at 0.015. Across the 23-year period studied, the growing season for these forests has lengthened by 6.5 days. Further, our analysis indicates a moderate correlation between the North Atlantic Oscillation and the season's start, alongside a slight correlation with its end. The most pronounced phenological shift was noted at the season's outset, yet comprehensive analysis underscores the broader trend of significant phenological changes, affirming the impact of climate change on the rhythm of Hessian forests.

1 Introduction

Human-caused climate change has damaged nature and people due to rapid changes in the atmosphere and biosphere [Intergovernmental Panel on Climate Change, 2023]. As an example, the global surface temperature over land in the last two decades was 1.59°C higher than in 1850–1900 [Intergovernmental Panel on Climate Change, 2023]. This warming trend affects the phenology of plants, including leaf-out and abscission [Richardson et al., 2013].¹ Higher temperatures have led to an earlier leaf burst, thus altering the timing of phenology [Bao et al., 2021, Jeong et al., 2011]. However, the impacts of climate change on phenology, such as altered growing seasons, create a feedback loop that can further influence the climate, due to its effect on the carbon cycle [Piao et al., 2008]. An adequate estimation of the changing phenology will be crucial to calculate climate models with altered carbon cycles and changing temperature [Richardson et al., 2013]. Because of this, an accurate estimation of the start of the season (SoS), the end of the season (EoS), and the length of the growing period is essential [Richardson et al., 2013]. Numerous studies in different countries have shown that climate change impacts result in an earlier SoS [Bao

et al., 2021, Dai et al., 2021, Bhutto et al., 2019, Jeong et al., 2011]. Yet, changes to the EoS have been less analyzed than the SoS [Richardson et al., 2013], although the EoS could be more significant for the extension of the growing season [Garonna et al., 2014]. Furthermore, there are interesting effects of the SoS and the North Atlantic Oscillation (NAO) on the EoS [Gouveia et al., 2008, Keenan and Richardson, 2015]. For example, an earlier SoS can result in an earlier EoS [Fu et al., 2014]. Because of this, we will take a closer look at the effects of the NAO and the SoS on the EoS in Hessian deciduous broadleaf forests. The estimation of SoS and EoS for large areas is possible with satellite data using the Normalized Difference Vegetation Index (NDVI)² [Testa et al., 2018] as we did in this study. Our research questions are: 1) Is there a significant impact of SoS on EoS? and 2) What is the effect of the NAO on the timing of SoS and EoS in Hessian deciduous broadleaf forest? In light of climate change, we will also try to 3) estimate how many days earlier leaf emergence occurs (SoS) and 4) how huge the expansion of the growing season is. Departing from previous studies, we strongly emphasize an expansion of the growing season, an

¹Phenology is defined as the study of the timing of recurrent biological events, the causes of their timing with regard to biotic and abiotic forces, and the interrelation among phases of the same or different species [Lieth, 1974].

²The normalized difference vegetation index, which is determined as the ratio of the difference between the near-infrared reflectance and the red visible reflectance to their sum, is usually used as an indicator of the green state of the vegetation and the photosynthetic activity [Myneni et al., 1995]

earlier SoS within the years, a significant effect of SoS on EoS, and a slight effect of the NAO on EoS.

2 Materials and Methods

2.1 Data

The study utilized Normalized Difference Vegetation Index (NDVI) data obtained from the MODIS satellite [DAAC, 2000-2023a]. This dataset covers a period from 2000 to 2023, with a spatial resolution of 250 meters and a temporal resolution of 16 days as recommended by Testa et al. [2018] for SoS and EoS calculation, covering the region of Hesse. Additionally, the MODIS VI Quality Layer was used to evaluate the quality of each pixel with the same temporal and spatial resolution [DAAC, 2000-2023b]. This step was critical for removing low-quality pixels and filtering out data affected by snow, clouds, and other atmospheric disturbances. Alongside with the NDVI data, CORINE land cover datasets for the years 2000, 2006, 2012, and 2018 were acquired [Service, 2000/2006/2012/2018]. These datasets provide detailed land cover information for Hesse at a resolution of 100 meters.

2.2 Research Area

Our research focuses on the Hessian region of Germany, situated in the center of the country. Hesse is characterized by its varied topography, which includes the low-lying areas around the Rhine and Main rivers in the south, as well as the more elevated terrains of the Odenwald also in the south, Taunus in the south west, the Westerwald and foothills of the Rothaar mountains in the west, and the Vogelsberg in the center. Hesse's climate is predominantly temperate, with varying weather patterns influenced by its geographical diversity. The region's vegetation is a mix of deciduous broadleaf forests, comprising mainly beech and oak, alongside coniferous forests, agricultural fields, and urban parklands [Hessisches Landesamt für Naturschutz, 2012]. Our study focused exclusively on areas classified as broad-leaved deciduous forests in Hesse in the Corine datasets [Service, 2000/2006/2012/2018]. To maintain consistency in temporal analysis, pixels that were consistently classified under this category at all four available CORINE time points (2000, 2006, 2012, and 2018) were selected. This consistent classification ensures the analysis of undisturbed forest areas over the study period [Jeganathan et al., 2014]. The initial step of the workflow involved resampling of the Corine land cover layers from their original 100-meter resolution to match the 250-meter resolution of the MODIS NDVI data. This resampling

was necessary for direct comparison and integration of the two datasets. Following resampling, a strict selection criterion was applied, where only pixels that remained 100% classified as broad-leaved deciduous forest were retained. This step was crucial to eliminate any border pixels that might have been affected by mixed land cover types due to the resolution change, thereby ensuring the purity of the forest data in the analysis. This layer was then used to remove all NDVI pixels that were not identified as deciduous broadleaf forest throughout each time step. Figure 1 shows 323,415 pixels which were consistently classified as broad-leaved deciduous forests, notably within the Odenwald, Taunus, and Westerwald areas in the west and south of Hesse.

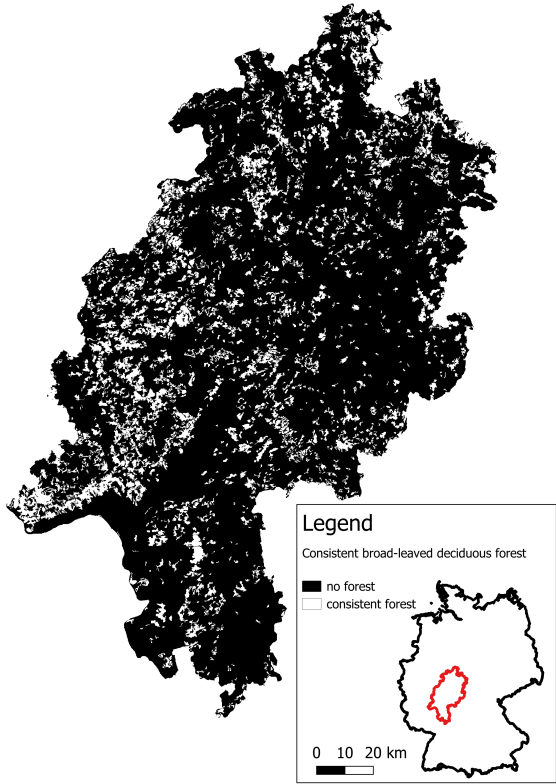


Figure 1: Map of pixels (323,415) that were consistently classified as broad-leaved deciduous forests in Hesse in the Corine datasets over all four different time points.

2.3 Data Preprocessing

The 323,415 pixels identified as consistently classified as broad-leaved deciduous forests collectively account for approximately 18.6 million different NDVI observations over the time span from 2000 to 2023. To ensure the accuracy and reliability of our dataset, the VI Quality layer was used to further refine the pixel data, excluding any observations

that did not meet the specified quality thresholds shown in Figure 2. This additional filtering step resulted in approximately 18 million NDVI observations being retained for further analysis. We used the VI Quality layer to identify NDVI observations which are most probably clouds, to then linear interpolate these values. Before hand we removed all pixels that had two consecutive cloud observations in a row, to reduce interpolation errors.

In the next step we employed the Savitzky-Golay filter for smoothing our NDVI data and reduce the impact of NDVI drops due to clouds or other disturbances when did not detect yet. Renowned for its ability to effectively smooth fluctuations while preserving critical features such as peak heights and widths, the Savitzky-Golay filter was deemed ideal for our study [Yuan et al., 2014, Bhutto et al., 2019]. We selected a polynomial order of 3 and a window size of 11 data points ($p = 3, n = 11$) for the filter recommended by Chen et al. [2004]. The parameters were tested and carefully chosen to optimize the balance between smoothing effectiveness and the preservation of important data characteristics.

Following, we implemented an additional threshold-based filtering step. We removed roughly 500,000 thousand pixel observations that exhibited NDVI values lower than 0.3. This decision was grounded in the assumption that, even during winter months, NDVI values seldom fall below this threshold. Consequently, values under 0.3 were considered anomalies, likely resulting from clouds or other extraneous factors, rather than genuine vegetative changes.

In our data processing workflow, we took the decisive step of completely removing pixels that exhibited NDVI values higher than 0.65 during the winter months in five or more different years. This threshold was meticulously chosen based on the understanding that such high NDVI values in winter are not characteristic of broad-leaved deciduous forests, which typically show reduced vegetative activity during this season [U.S. Geological Survey, 2023]. Instead, these high values suggest the presence of coniferous forests, which retain their foliage and, consequently, maintain higher NDVI values throughout the year. By eliminating these pixels, we aimed to refine our analysis to focus exclusively on broad-leaved deciduous forests, ensuring the specificity and accuracy of our study's focus on vegetation dynamics within this particular forest type. After these two steps we filtered out years of pixels lacking at least one NDVI value for any month from March through October, leading to the retention of about 15.7 million NDVI observations for in-depth analysis. This exclusion was vital to ensure the reliability of our calculations for the start and end of the growing season, which depend heavily on the presence of data points across

the essential months. The absence of comprehensive data coverage during this period would lead to inaccuracies in identifying the vegetative period's beginning and end, thus risking the validity of our conclusions.

In our analysis, we expanded our dataset to include a series of daily dates for each year, tailored specifically from the first to the last NDVI observation of each pixel annually. Following this, we applied linear interpolation equal to Jeganathan et al. [2014], to populate missing NDVI values across these tailored date ranges for each pixel. By adopting this method, we were able to construct a seamless and coherent time series of NDVI values for every pixel for each year and day. This process was instrumental in enabling a more precise and nuanced examination of the start and end of season over time.

Bits	Parameter Name	Value Description
0-1	VI Quality (MODLAND QA Bits)	00 VI produced with good quality 01 VI produced, but check other OA 10 Pixel produced, but most probably cloudy 11 Pixel not produced due to other reasons than clouds
2-5	VI Usefulness	0000 Highest quality 0001 Lower quality 0010 Decreasing quality 0100 Decreasing quality 1000 Decreasing quality 1001 Decreasing quality 1010 Decreasing quality 1100 Lowest quality 1101 Quality so low that it is not useful 1110 L1B data faulty 1111 Not useful for any other reason/not processed
6-7	Aerosol Quantity	00 Climatology 01 Low 10 Intermediate 11 High
8	Adjacent cloud detected	0 No 1 Yes
9	Atmosphere BRDF Correction	0 No 1 Yes
10	Mixed Clouds	0 No 1 Yes
11-13	Land/Water Mask	00 Shallow Ocean 01 Land (Nothing else but land) 010 Ocean coastlines and lake shorelines 011 Shallow inland water 100 Ephemeral water 101 Deep inland water 110 Moderate or continental ocean 111 Deep ocean
14	Possible snow/ice	0 No 1 Yes
15	Possible shadow	0 No 1 Yes

Figure 2: Descriptions of the VI Quality Assessment Science Data Sets, all yellow marked binary's were filtered out [Kamel Didan and Armando Barreto Munoz, 2024]

2.4 Calculation of SoS and EoS

To determine the start and end of the growing season within our study, we first normalized the NDVI values for each pixel across the entire dataset. This normalization involved calculating the global minimum and maximum NDVI values for each pixel and adjusting all NDVI readings to a scale from 0 to 1,

based on these global extremes. This method was recommended by Wu et al. [2017].

For identifying the SoS, we analyzed the normalized NDVI time series for each pixel-year combination, looking for the first instance where the NDVI value exceeded a threshold of 0.5 for at least three consecutive days [Jeganathan et al., 2014]. This approach allowed us to pinpoint the onset of significant vegetative growth, marking the start of the growing season.

To calculate the EoS, we first determined the date of peak NDVI for each pixel in a given year, representing the maximum vegetative biomass. From this peak, we then examined the subsequent NDVI time series, identifying the first occurrence where NDVI values fell below the 0.5 threshold for three consecutive days, post the peak NDVI date. This methodology was deployed to accurately capture vegetative decline, signaling the end of the growing season.

By meticulously following these steps, we were able to generate comprehensive datasets delineating the SoS and EoS for each pixel across the study area for every year. This data forms the backbone of our analysis, enabling a detailed exploration of vegetative dynamics and seasonal growth patterns across the broad-leaved deciduous broadleaf forests of Hesse.

2.5 Statistics

For our analysis, we focused exclusively on pixels with data spanning a minimum of 20 different years, excluding outliers such as observations where SoS or EoS fell outside the typical phenological window. Specifically, if SoS or EoS was recorded in January, February, June, July, August, or December, those data points were removed to ensure the accuracy and relevance of our findings. Our analysis covered 539,457 observations across 24,094 pixels, providing a substantial dataset for examining phenological changes.

For the analysis of linear trends between the year and the Start-/End of Season and length of growing season for each pixel, we employed Robust Linear Regression (RLM). This statistical method was chosen due to its resilience against outliers, which are common in ecological datasets like ours, where variations in pixel data can result from numerous factors such as atmospheric conditions, sensor errors, or changes in land use. RLM provides a more accurate estimation of trends by minimizing the influence of these outliers, ensuring that our analysis reflects the underlying patterns in the data rather than being skewed by anomalies.

For examining the correlations between SoS and EoS, and the impact of the NAO on SoS and EoS, we employed Pearson's correlation coefficient. This

choice was based on visual assessments confirming a normal distribution of our data, which is a requirement for the valid application of Pearson's correlation. Additionally, the large size of our dataset further mitigates potential risks associated with deviations from normality. For the analysis of the correlation between the NAO and the SoS as well as the EoS, we calculated the mean NAO values over the 90 days preceding each pixel's SoS and EoS dates. This approach allowed us to capture the climatic influence of the NAO on phenological timings of SoS and EoS.

2.6 R

In this study, we used a number of different R packages for data manipulation, analysis, and visualization. Date and time manipulations were handled using '*lubridate*' [Grolemund and Wickham, 2021], while string operations were streamlined with '*stringr*' [Wickham, 2019]. The '*dplyr*' [Wickham et al., 2021] and '*tidyverse*' [Wickham and Henry, 2021] packages facilitated data cleaning and tidying, ensuring a structured dataset for analysis. For linear interpolation, '*zoo*' [Zeileis and Grothendieck, 2020] was used. Spatial data analysis was conducted using '*sf*' [Pebesma, 2018], allowing for effective manipulation and visualization of spatial features. For visualization, '*ggplot2*' [Wickham, 2021] was used, with additional support from '*scales*' [Wickham and Seidel, 2021] for scale customization. The '*patchwork*' package [Pedersen, 2020] enabled the seamless combination of plots. Statistical analyses, including linear and non-linear modeling, were supported by '*MASS*' [Venables and Ripley, 2002]. To ensure a consistent analysis environment across different systems, the '*envimaR*' package [Reudenbach et al., 2021] was essential.

3 Results

Table 1 shows the occurrences of SoS and EoS across all months. The main peak for SoS is observed in April with 367,296 instances, indicating the primary onset of the growth season. For EoS, October marks the peak with 384,648 instances. Outliers in the data, identified in the months of January, February, June, July, August, and December, cumulatively account for 24,044 SoS and 30,951 EoS instances. Additionally, observations categorized as NA total 63 for SoS and 22,263 for EoS, reflecting data that could not be assigned to a specific month.

In the case of the SoS, a significant trend towards earlier dates was observed in 6.217% of pixels, with the slope among these significant pixels

being -0.701 days per year. This indicates an advancement of approximately 7.01 days per decade for these pixels. Across the entire dataset, the average trend was a more modest advancement of -0.182 days per year. For the End of Season, 2.258% of pixels showed a statistically significant trend towards later dates, with a slope of 0.456 days per year among these pixels. This reflects a delay of about 4.56 days per decade in EoS. When all pixels were considered, the delay was less pronounced, with a slope of 0.108 days per year. Figure 3 shows these trends visually.

The relationship between SoS and EoS exhibited a slightly positive correlation (correlation coefficient = 0.015, p -value $< 2.2 \times 10^{-16}$), suggesting a minimal tendency for earlier EoS dates to follow earlier SoS dates.

Investigating the effect of the NAO on phenological timings revealed that NAO values, averaged over the 90 days before each pixel's SoS and EoS, had a moderate negative correlation with SoS ($r = -0.303$, p -value $< 2.2 \times 10^{-16}$) and a slight positive correlation with EoS ($r = 0.068$, p -value $< 2.2 \times 10^{-16}$). This indicates that higher NAO values generally precede earlier SoS and slightly influence EoS timings.

Our findings also highlighted an expansion of the growing season across the study area. Pixels with significant trends showed an increase of 11 days per decade (slope: 1.104 days per year), while the broader analysis across all pixels suggested a more conservative extension of 2.8 days per decade (slope: 0.283 days per year).

These results collectively provide a comprehensive overview of the phenological changes occurring across the study area, revealing the timing and trends of vegetation cycles over the years.

Table 1: Distribution of SoS and EoS by month over all years. NA values indicate years of pixels where the SoS or EoS calculation thresholds were never exceeded.

Month	SoS Count	EoS Count
January	21992	5
February	9748	7
March	291886	4
April	367296	12
May	19521	46
June	247	1310
July	42	3461
August	15	2483
September	5	32116
October	7	384648
November	1	242285
December	0	22181
NA	63	22263

4 Discussion

Due to climate change and warmer temperatures in winter and early spring, the SoS has advanced [Bhutto et al., 2019, Liu et al., 2016, Bórnez et al., 2021]. This shift in deciduous broadleaf forests in Hesse has also been documented in this study. The primary driver of this shift is higher preseason temperatures [Bórnez et al., 2021]. In some regions, climate change may lead to drier conditions, potentially delaying the SoS [Bhutto et al., 2019]; however, this has not been observed in Hesse. The shift in SoS across all pixels is 1.82 days per decade, placing it on the lower range of shifts reported in various studies summarized in [Jeganathan et al., 2014]. 6.217% of these pixels have been significant, exhibiting an advancement of 7.01 days per decade, which falls within the upper range of SoS shifts found in the literature [Jeganathan et al., 2014]. Jeong et al. [2011] identified a decreasing trend in SoS advancement and EoS delay between 2000 to 2008 compared to 1982 to 1999, due to a smaller temperature increase in the later time span in the Northern Hemisphere. This observation could also apply to our analysis for the first decade, starting in 2000. Other studies anticipate a later EoS due to higher temperatures in autumn. Our findings are similar, but the extension of the EoS was not as strong as the advancement of the SoS, in contrast to other studies[Jeganathan et al., 2014]. The advancing SoS and the delaying EoS concurs with other results predicting a correlation between the SoS and the EoS [Keenan and Richardson, 2015]. But Keenan and Richardson [2015] noted that if the SoS begins approximately one day earlier, it shifts the EoS by 0.6 days earlier as well, suggesting the growing season may not extend as much as models based primarily on temperature changes would predict. In our analysis, an earlier SoS was associated with a marginally earlier EoS, consistent with other literature [Liu et al., 2016]. The influence of the SoS on the EoS was analyzed by Keenan and Richardson [2015], who categorized the impact into direct and indirect factors [Keenan and Richardson, 2015]. Direct factors could include programmed cell death, while indirect factors might involve an increased likelihood of drought or insect outbreaks following an earlier SoS [Keenan and Richardson, 2015]. Another hypothesis suggests that an earlier EoS could occur when trees reach their carbon sink capacity sooner due to an advancing SoS [Fu et al., 2014]. Nonetheless, our findings suggest only a slight correlation of 0.015 between the SoS and the EoS. Interestingly, another study found a negative effect of the SoS on the EoS in deciduous broadleaf forests [Liu et al., 2016]. Using the Savitzky-Golay smoother with different parameters, we also observed a slight negative correlation between the SoS

Comprehensive Analysis of SoS and EoS Trends ($p \leq 0.05$)

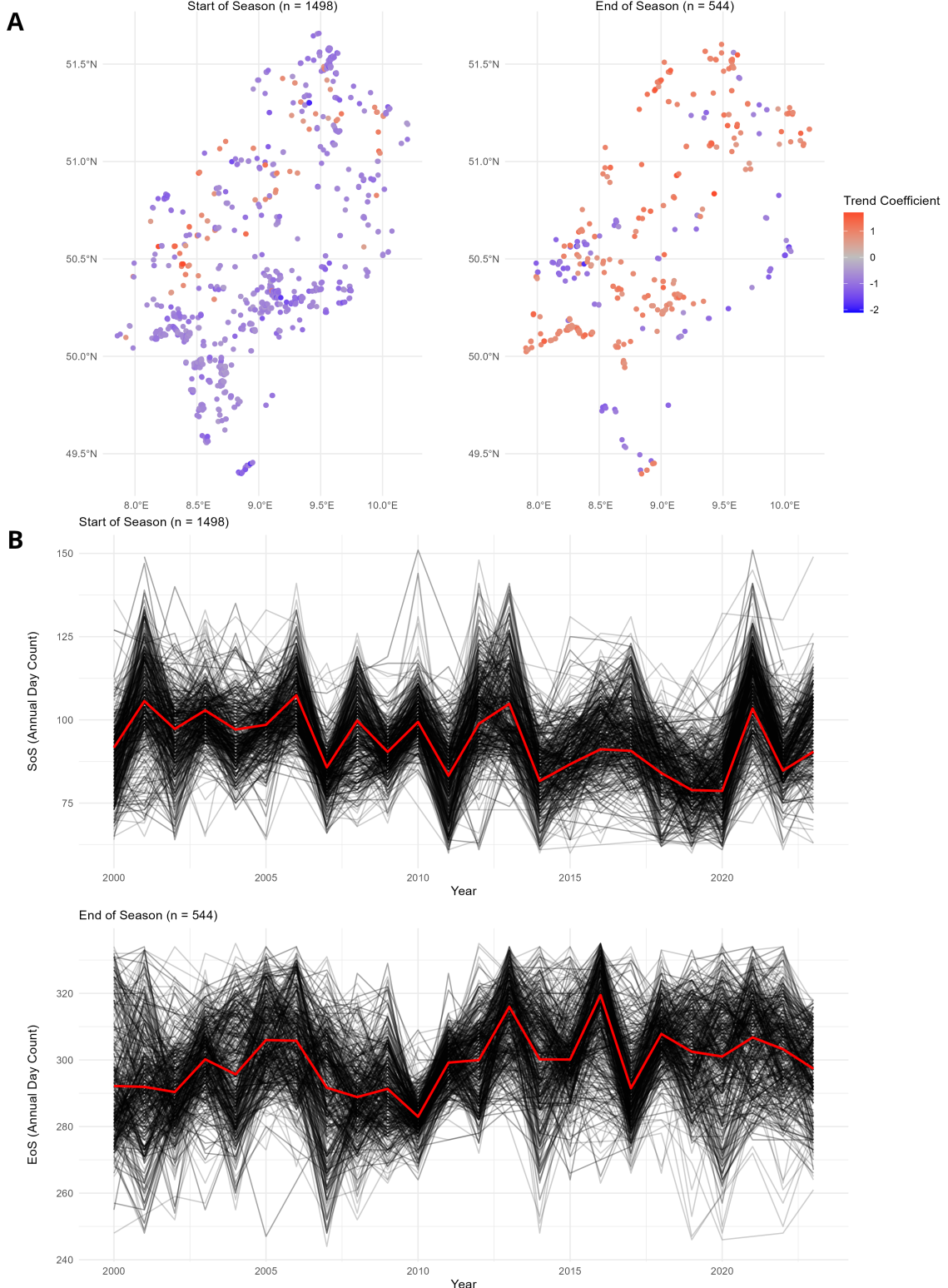


Figure 3: **A:** Slope of significant linear trends of SoS ($n = 1498$) and EoS ($n = 544$). **B:** Significant trends of SoS and EoS of over the years for each pixel. Both focusing exclusively on pixels with SoS or EoS recordings in at least 20 distinct years from 2000 to 2023

and EoS. Without a clear explanation, the effect of a later SoS resulting in a marginally earlier EoS warrants further investigation. One hypothesis is that a colder year could lead to both a later SoS and an earlier EoS. That temperature is the main influence on the SoS and EoS in deciduous broadleaf forests [Linderholm, 2006, Bórnez et al., 2021] supports this notion. Furthermore, there is a notable correlation between the NAO and the SoS. Higher NAO values, associated with increased winter temperatures, lead to an advanced SoS in northeast Europe [Gouveia et al., 2008]. Conversely, on the Iberian Peninsula, lower NAO values result in more winter rainfall, thereby advancing the SoS and affecting NDVI values [Gouveia et al., 2008]. In our study the influence of NAO on the EoS, with a correlation of 0.068, is less pronounced than its impact on the SoS. Nevertheless, this slight correlation suggests that a high NAO 90 days before the EoS could delay it. However, given the slight correlation and despite a very low p-value, we found no evidence of a huge impact of the NAO on the EoS. Further research into the influence of the NAO on climate variables and the SoS/EoS in deciduous broadleaf forests is needed for conclusive statements. Nevertheless, the NAO showed a moderate correlation with the SOS, which emphasises the importance of the NAO for the phenology of deciduous forests in Hesse. The expansion of the growing season aligns with other scientific papers [Linderholm, 2006]. Across all pixels, we observed a mean expansion of 2.83 days per decade, with 1691 pixels showing significance with a mean expansion of 11 days per decade. This extension of the vegetation period could alter the carbon cycle, as more time is available for photosynthesis, which would have a positive effect on the function of forests as carbon sinks. [Linderholm, 2006]. However, this optimistic perspective is eased by considerations from Piao et al. (2008), who noted that warmer temperatures during autumn might increase CO₂ emissions from ecosystems. Consequently, the efficacy of forests as carbon sinks in light of a prolonged growing season becomes a complex interplay between enhanced photosynthetic activity and increased CO₂ emissions, underscoring the complex relationship between climate change, vegetation phenology, and carbon dynamics.

As cited by Jeganathan et al. [2014], the range of findings regarding the changing SoS and EoS across scientific papers for the Northern Hemisphere exhibits significant variance. Similarly, in our study, we observed variations in the SoS and EoS depending on the calculation methods employed. Due to this, we would like to highlight some limitations of the study's scope.

5 Limitations

The calculation of SoS and EoS was central to our research, underscoring the importance of accurately determining these variables. Several methods are available to calculate the SoS and the EoS, each with its implications for the results [Wu et al., 2017]. We found that the choice of calculation method significantly influences the SoS and EoS outcomes, affecting the correlation results. The local threshold method for each year is considered among the most reliable for determining SoS and EoS [Wu et al., 2017]. Yet, this approach only showed a correlation of 0.28 with ground measurements [Wu et al., 2017]. Additionally, our analysis revealed that the choice of filtering method can significantly alter regression outcomes. It is therefore essential to discern whether cloudy pixels have been interpolated and which filters and parameters have been employed to smooth the NDVI time series. For instance, varying the application of the Savitzky-Golay filter yielded slight negative or positive correlations between SoS and EoS. Although we applied rigorous filtering to calculate using the highest quality pixels, less stringent filtering and preprocessing of our time series led to weaker correlations. The exclusion of outliers and the selection criteria for the minimum number of years per pixel also influenced the trend of shifting or delaying SoS and EoS.

Given the profound impact of different filtering methods and calculation options on SoS and EoS, we advocate for diverse yet transparent calculation approaches, as seen in prior studies [Wu et al., 2017, Bao et al., 2021, Liu et al., 2016]. Despite the variety in methods, all resulted in a shift of the SoS and a delay in the EoS, indicating a consistent pattern of phenological change in deciduous broadleaf forests in Hesse, albeit with varying degrees of significance. For this reason, the exact values should be treated with caution, but the general trends in SoS, EoS, the length of the growing season and the influence of the NAO on the phenology of deciduous forests in Hesse are clear.

6 Conclusion

Utilizing NDVI data from MODIS, this study confirms an advancing SoS in deciduous broadleaf forests in Hesse from 2000 to 2023, with an average shift of approximately 1.66 days per decade and an even more pronounced 7.07 days per decade for all significant pixels (6.2%). Conversely, the EoS exhibited a less distinct but nonetheless delaying trend of 0.96 days per decade across all pixels, with significant pixels (2.3%) experiencing a delay of 3.84 days per decade. These findings are consistent with other research on deciduous broadleaf forests

in the northern hemisphere, highlighting similar trends in EoS and SoS timing [Bórnez et al., 2021]. Unlike some studies that reported a correlation between SoS and EoS, our analysis only identified a slight positive correlation.

Additionally, in line with existing literature, we observed a correlation between the North Atlantic Oscillation (NAO) and both SoS and EoS. Elevated NAO values during winter and spring correlated with an earlier SoS, likely due to increased winter temperatures. However, the impact of NAO on EoS was less definitive, with a correlation coefficient of 0.068.

Over 23 years, the growing season lengthened by 6.5 days, with 7% of pixels showing significant expansion, potentially affecting the carbon cycle in deciduous broadleaf forests in Hesse.

Our research adds to the growing body of evidence highlighting the impact of anthropogenic climate change on the phenology of deciduous broadleaf forests, including those in Hesse. This underscores the broader implications of global warming and changing phenological patterns.

References

- Gang Bao, Hugejiletu Jin, Siqin Tong, Jiquan Chen, Xiaojun Huang, Yuhai Bao, Changliang Shao, Urtnasan Mandakh, Mark Chopping, and Lingtong Du. Autumn phenology and its covariation with climate, spring phenology and annual peak growth on the mongolian plateau. *Agricultural and Forest Meteorology*, 298-299: 108312, 2021. ISSN 0168-1923. doi: <https://doi.org/10.1016/j.agrformet.2020.108312>. URL <https://www.sciencedirect.com/science/article/pii/S0168192320304147>.
- Sarfaraz Ali Bhutto, Xiaoyue Wang, and Jian Wang. The start and end of the growing season in pakistan during 1982–2015. *Environmental Earth Sciences*, 78(133), 2019. doi: 10.1007/s12665-019-8135-1.
- Kevin Bórnez, Aleixandre Verger, Adrià Descals, and Josep Peñuelas. Monitoring the responses of deciduous forest phenology to 2000–2018 climatic anomalies in the northern hemisphere. *Remote Sensing*, 13(14):2806, 2021. doi: 10.3390/rs13142806. URL <https://doi.org/10.3390/rs13142806>. Special Issue: Advanced Phenology, and Land Cover and Land Use Change Studies.
- Jin Chen, Per. Jönsson, Masayuki Tamura, Zhi-hui Gu, Bunkei Matsushita, and Lars Eklundh. A simple method for reconstructing a high-quality ndvi time-series data set based on the savitzky–golay filter. *Remote Sensing of Environment*, 91(3):332–344, 2004. ISSN 0034-4257. doi: <https://doi.org/10.1016/j.rse.2004.03.014>. URL <https://www.sciencedirect.com/science/article/pii/S003442570400080X>.
- NASA LP DAAC. Mod13q1.061 – ndvi 16-day l3 global 250m, 2000-2023a. URL <https://lpdaac.usgs.gov/products/mod13q1v061/>. Accessed on 01-5-2024.
- NASA LP DAAC. Mod13q1.061 – vi quality 16-day l3 global 250m, 2000-2023b. URL <https://lpdaac.usgs.gov/products/mod13q1v061/>. Accessed on 01-5-2024.
- Junhu Dai, Mengyao Zhu, Wei Mao, Ronggao Liu, Huanjiang Wang, Juha Mikael Alatalo, Zexing Tao, and Quansheng Ge. Divergent changes of the elevational synchronicity in vegetation spring phenology in north china from 2001 to 2017 in connection with variations in chilling. *International Journal of Climatology*, 41(13):6109–6121, 2021. doi: 10.1002/joc.7170. Funding information: National Key R D Program of China, Grant/Award Number: 2018YFA0606102; National Natural Science Foundation of China, Grant/Award Number: 41771056; Strategic Priority Research Program of Chinese Academy of Sciences, Grant/Award Number: XDA19020303.
- Yongshuo S. H. Fu, Matteo Campioli, Yann Vitasse, Hans J. De Boeck, Joke Van den Berge, Hamada AbdElgawad, Han Asard, Shilong Piao, Gaby Deckmyn, and Ivan A. Janssens. Variation in leaf flushing date influences autumnal senescence and next year’s flushing date in two temperate tree species. *Proceedings of the National Academy of Sciences*, 111(20):7355–7360, May 2014. doi: 10.1073/pnas.1321727111. URL www.pnas.org/cgi/doi/10.1073/pnas.1321727111.
- Irene Garonna, Rogier de Jong, Allard J.W. de Wit, Caspar A. Mücher, Bernhard Schmid, and Michael E. Schaepman. Strong contribution of autumn phenology to changes in satellite-derived growing season length estimates across europe (1982–2011). *Global Change Biology*, 20: 3457–3470, November 2014. doi: 10.1111/gcb.12625.
- Célia Gouveia, Ricardo M. Trigo, Carlos C. DaCamarra, Renata Libonati, and José M. C. Pereira. The north atlantic oscillation and european vegetation dynamics. *International Journal of Climatology*, 28:1835–1847, 2008. doi: 10.1002/joc.1682.
- Garrett Grolemund and Hadley Wickham. *lubridate: Make Dealing with Dates a Little Easier*, 2021. URL <https://CRAN.R-project.org/package=lubridate>. R package version 1.7.10.

- Umwelt und Geologie (HLNUG) Hessisches Landesamt für Naturschutz. Facetten des waldes; der hessische wald in zahlen, grafiken und text vergleich 1994 und 2009, 2012. URL https://www.hlnug.de/fileadmin/dokumente/naturschutz/shop/Schriften_Naturschutz_601.pdf.
- Intergovernmental Panel on Climate Change. Summary for policymakers. in: Climate change 2023: Synthesis report. contribution of working groups i, ii and iii to the sixth assessment report, 2023.
- C. Jeganathan, J. Dash, and P.M. Atkinson. Remotely sensed trends in the phenology of northern high latitude terrestrial vegetation, controlling for land cover change and vegetation type. *Remote Sensing of Environment*, 143:154–170, 2014.
- Su-Jong Jeong, Chang-Hoi Ho, Hyeyon-Ju Gim, and Molly E. Brown. Phenology shifts at start vs. end of growing season in temperate vegetation over the northern hemisphere for the period 1982–2008. *Global Change Biology*, 17(7):2385–2399, 2011. ISSN 1354-1013. doi: 10.1111/j.1365-2486.2011.02397.x. URL <https://onlinelibrary.wiley.com/doi/abs/10.1111/j.1365-2486.2011.02397.x>. Special Issue on Advances of Ecological Remote Sensing Under Global Change.
- Kamel Didan and Armando Barreto Munoz. *MODIS Collection 6.1 (C61) VegetationIndex Product UserGuide*. NASA Earth Observing System Data and Information System (EOSDIS) Land Processes (LP) Distributed Active Archive Center (DAAC), 2024. URL https://lpdaac.usgs.gov/documents/621/MOD13_User_Guide_V61.pdf. Accessed on 02-06-2024.
- Trevor F. Keenan and Andrew D. Richardson. The timing of autumn senescence is affected by the timing of spring phenology: implications for predictive models. *Global Change Biology*, 21:2634–2641, 2015. doi: 10.1111/gcb.12890.
- Helmut Lieth. *Phenology and Seasonality Modeling*, volume 8. 1974. doi: <https://doi.org/10.1007/978-3-642-51863-8>.
- Hans W. Linderholm. An increasing number of studies have reported on shifts in timing and length of the growing season, based on phenological, satellite and climatological studies. *Agricultural and Forest Meteorology*, 137(1-2):1–14, 2006. doi: 10.1016/j.agrformet.2006.03.006. Review.
- Qiang Liu, Yongshuo H. Fu, Zaichun Zhu, Yongwen Liu, Zhuo Liu, Mengtian Huang, Ivan A. Janssens, and Shilong Piao. Delayed autumn phenology in the northern hemisphere is related to change in both climate and spring phenology. *Global Change Biology*, 22:3702–3711, 2016. doi: 10.1111/gcb.13311.
- R.B. Myneni, F.G. Hall, P.J. Sellers, and A.L. Marshak. The interpretation of spectral vegetation indexes. *IEEE Transactions on Geoscience and Remote Sensing*, 33(2):481–486, Mar 1995. doi: 10.1109/36.377948. Indexed on 1995-03-01.
- Edzer Pebesma. *Simple Features for R*, 2018. URL <https://CRAN.R-project.org/package=sf>.
- Thomas Lin Pedersen. *patchwork: The Composer of Plots*, 2020. URL <https://CRAN.R-project.org/package=patchwork>. R package version 1.1.1.
- S. Piao, P. Ciais, P. Friedlingstein, et al. Net carbon dioxide losses of northern ecosystems in response to autumn warming. *Nature*, 451:49–52, 2008. doi: 10.1038/nature06444.
- Christoph Reudenbach, Thomas Nauss, and Marvin Ludwig. envimr: Utility functions to configure standard project environments in labs, 2021. URL <https://github.com/envima/envimr.R>.
- Andrew D. Richardson, Trevor F. Keenan, Mirco Migliavacca, Youngryel Ryu, Oliver Sonnentag, and Michael Toomey. Climate change, phenology, and phenological control of vegetation feedbacks to the climate system. *Agricultural and Forest Meteorology*, 169: 156–173, 2013. ISSN 0168-1923. doi: <https://doi.org/10.1016/j.agrformet.2012.09.012>. URL <https://www.sciencedirect.com/science/article/pii/S0168192312002869>.
- Copernicus Land Monitoring Service. Corine land cover, 2000/2006/2012/2018. URL <https://land.copernicus.eu/en/products/corine-land-cover>. Accessed on 02-06-2024.
- S. Testa, K. Soudani, L. Boschetti, and E. Borgogno Mondino. Modis-derived evi, ndvi and wdrvi time series to estimate phenological metrics in french deciduous forests. *International Journal of Applied Earth Observation and Geoinformation*, 64:132–144, 2018.
- U.S. Geological Survey. Ndvi, the foundation of remote sensing phenology. <https://www.usgs.gov/special-topics/remote-sensing-phenology/science/ndvi-foundation-remote-sensing-phenology>, 2023. Accessed: 2023-03-18.

W. N. Venables and B. D. Ripley. *Modern Applied Statistics with S*, 2002. URL <https://www.stats.ox.ac.uk/pub/MASS4>. ISBN 0-387-95457-0.

Hadley Wickham. *stringr: Simple, Consistent Wrappers for Common String Operations*, 2019. URL <https://CRAN.R-project.org/package=stringr>. R package version 1.4.0.

Hadley Wickham. *ggplot2: Create Elegant Data Visualisations Using the Grammar of Graphics*, 2021. URL <https://CRAN.R-project.org/package=ggplot2>. R package version 3.3.5.

Hadley Wickham and Lionel Henry. *tidyverse: Tidy Messy Data*, 2021. URL <https://CRAN.R-project.org/package=tidyr>. R package version 1.1.3.

Hadley Wickham and Dana Seidel. *scales: Scale Functions for Visualization*, 2021. URL <https://CRAN.R-project.org/package=scales>. R package version 1.1.1.

Hadley Wickham, Romain François, Lionel Henry, and Kirill Müller. *dplyr: A Grammar of Data Manipulation*, 2021. URL <https://CRAN.R-project.org/package=dplyr>. R package version 1.0.7.

Chaoyang Wu, Dailiang Peng, Kamel Soudani, Lukas Siebicke, Christopher M. Gough, M. Altaf Arain, Gil Bohrer, Peter M. Lafleur, Matthias Peichl, Alemu Gonsamo, Shiguang Xu, Bin Fang, and Quansheng Ge. Land surface phenology derived from normalized difference vegetation index (ndvi) at global fluxnet sites. *Agricultural and Forest Meteorology*, 233:171–182, 2017. Contents lists available at ScienceDirect.

Fei Yuan, Cuizhen Wang, and Martin Mitchell. Spatial patterns of land surface phenology relative to monthly climate variations: Us great plains. *GIScience & Remote Sensing*, 51(1):30–50, 2014. ISSN 1548-1603 (Print) 1943-7226 (Online). doi: 10.1080/15481603.2014.883210. URL <https://doi.org/10.1080/15481603.2014.883210>.

Achim Zeileis and Gabor Grothendieck. *zoo: S3 Infrastructure for Regular and Irregular Time Series*, 2020. URL <https://CRAN.R-project.org/package=zoo>. R package version 1.8-8.